

Characterization of a UBXD1 Polymorphic Variant and Identification of UBXD1
Interacting Proteins

A Thesis
Submitted to
the Temple University Graduate Board

In Partial Fulfillment
Of the Requirements for the Degree
MASTER OF SCIENCE

By
Dane Brittan Kyle
May 2011

Thesis Approval(s):

Dale Haines, Ph.D., Thesis Advisor, Fels Institute
Xavier Graña, Ph.D., Thesis Committee Chair, Fels Institute
Carmen Sapienza, Ph.D., Fels Institute
Lawrence Goldfinger, Ph.D., Anatomy and Cell Biology

ABSTRACT

Title: Characterization of a UBXD1 Polymorphic Variant and Identification of UBXD1

Interacting Proteins

Candidate's Name: Dane Brittan Kyle

Degree: Master of Science

Temple University, 2011

M.S. Thesis Advisory Committee Chair: Xavier Graña, Ph.D.

p97, a member of the AAA ATPase (ATPases Associated with diverse cellular Activities) family of proteins, exists as a hexamer with two centrally located ATPase domains D1 and D2. The ATPase function of p97 is the means by which mechanical force is applied to substrates, consequently changing their conformation. As a highly abundant protein within cells, p97 has been shown to function in multiple pathways whereby specificity is directed via adaptor proteins. The largest family of *bona fide* p97 adaptors is the 'Ubiquitin regulatory X' (UBX) domain containing family of adaptors. In addition to the UBX domain containing family of adaptors, proteins containing a PUB domain have been implicated in binding to p97. The p97 adaptor protein UBXD1 contains both a UBX and PUB domain, however the UBX domain does not participate in binding p97 due to absence of the conserved motif required for binding. Recently, a highly conserved region within the first 150 amino acids of the UBXD1 N-terminus has been shown to participate in p97 binding (Kern et al., 2009).

The cellular function of UBXD1 remains largely unknown. One of the focuses of the Haines laboratory is to elucidate the function of UBXD1. Unpublished results from within the laboratory suggest UBXD1 to be defective at interacting with p97 mutants found in Inclusion Body Myopathy associated with Paget's Disease of Bone and Frontotemporal Dementia (IBMPFD) and Amyotrophic Lateral Sclerosis (ALS) disease, leading to a disruption of the autophagy pathway. These results suggest a role for UBXD1 as a human disease relevant protein. Search of a Single Nucleotide Polymorphism (SNP) database for polymorphisms within conserved regions of UBXD1 was carried out. Interestingly, the SNP database revealed a polymorphic variant within a conserved region of the PUB domain. The SNP was found within the asparagine residue of the evolutionarily conserved surface patch, resulting in an asparagine(N) to serine(S) substitution, termed N184S.

The two main objectives of my master's thesis project are 1) to characterize this UBXD1 polymorphic variant in terms of p97 binding capabilities and determine the prevalence of the N184S PUB domain SNP within the population and 2) identification/verification of UBXD1 interacting proteins that may provide a clue for UBXD1 function in autophagy and define domains required for association. As a result of interaction-based studies, I have been able to show a severe loss-of-binding phenotype by the UBXD1 N184S polymorphic variant. While the N184S PUB domain SNP could not be validated within my sample population, the interaction data led to the discovery of potential UBXD1 interacting proteins. Additionally, proteomics data generated by Dr. Dale Haines in the lab of Dr. Raymond Deshaies revealed ERGIC-53 to be a novel binding partner of UBXD1. Through interaction-

based studies, I have been able to determine the regions required for the interaction between UBXD1 and ERGIC-53 as well as propose a possible role for p97^{UBXD1} complexes in autophagy.

ACKNOWLEDGEMENTS

I would first like to thank my committee members for the advice and support they have provided to me throughout this entire process. Their dedication is and forever will be greatly appreciated. I would also like to thank Dr. Lawrence Goldfinger for his contributions in serving as an outside reviewer.

Additionally, I would like to thank the lab of Dr. Carmen Sapienza for providing access to the DNA samples used for genotyping the UBXD1 PUB domain and the lab of Dr. Xavier Graña and Dr. Judit Garriga for the use of their equipment and supplies in determining UBXD1 interacting proteins.

I would like to extend a special thanks to Dr. Dale Haines for the opportunity to participate in the masters program and study in his lab. Thanks to you, I have made great strides both personally and professionally.

A special thanks is also extended to those who wrote and/or spoke on my behalf in support of my application to dental school. With your help, I have achieved my goal and for that I am forever grateful.

Finally, I would like to thank my family and friends for the love and support they have given me throughout life's struggles and achievements. Each of you has helped mold me into who I am today. Words cannot express my gratitude and appreciation for all of you.

TABLE OF CONTENTS

	PAGE
ABSTRACT.....	ii
ACKNOWLEDGEMENTS.....	v
LIST OF FIGURES.....	ix
LIST OF TABLES.....	x
LIST OF ABBREVIATIONS.....	xi
CHAPTER	
1. INTRODUCTION.....	1
1.1 THE AAA ATPASE, p97 (VCP).....	1
1.2 THE 'UBIQUITIN REGULATORY X' DOMAIN.....	5
1.3 THE PEPTIDE:N-GLYCANASE UBX-CONTAINING PROTEINS (PUB) DOMAIN.....	6
1.4 UBXD1.....	6
1.5 ERGIC-53.....	7
1.6 RESEARCH FOCUS, HYPOTHESIS AND GOALS.....	8
2. MATERIALS AND METHODS.....	10
2.1 PLASMID PREPARATION.....	10
2.1.1 UBXD1 ^{FLAG} N184S.....	10
2.1.2 ^{FLAG} ERGIC-53.....	11
2.2 TISSUE CULTURE.....	11
2.2.1 H1299 AND 293T CELLS.....	11
2.2.2 pIND CELL LINE.....	12
2.2.3 miR-30 BASED CELL SYSTEM.....	12

2.3 TRANSFECTIONS.....	12
2.3.1 H1299 CELLS.....	12
2.3.2 293T CELLS.....	13
2.4 IMMUNOPRECIPITATIONS.....	13
2.4.1 FLAG IMMUNOPRECIPITATIONS (IP RIPA).....	13
2.4.2 FLAG IMMUNOPRECIPITATIONS (EBC).....	14
2.4.3 HA IMMUNOPRECIPITATIONS (EBC).....	15
2.5 WESTERN BLOTTING.....	15
2.6 PROTEIN GEL FIXING AND STAINING WITH COOMASSIE BRILLIANT BLUE.....	16
2.7 GENOTYPING OF THE UBXD1 PUB DOMAIN.....	16
2.8 PONAESTERONE INDUCIBLE SYSTEM.....	16
2.9 UBXD1 KNOCK-DOWN.....	17
3. RESULTS.....	18
3.1 LOSS OF BINDING PHENOTYPE WITH UBXD1 POLYMORPHIC VARIANT, UBXD1 N184S.....	18
3.2 DETERMINING THE FREQUENCY OF THE UBXD1 N184S POLYMORPHISM.....	22
3.3 ATTEMPTING TO IDENTIFY UBXD1 N184S INTERACTING PROTEINS BY MASS SPECTROSCOPY BASED PROTEOMICS.....	24
3.4 SOLUTION BASED PROTEOMICS REVEALS A NOVEL UBXD1 INTERACTING PROTEIN, ERGIC-53.....	29
3.5 VERIFICATION OF PROTEOMICS DATA BY WESTERN BLOT ANALYSIS.....	34
3.6 ERGIC-53 INTERACTS WITH THE UBXD1 N-TERMINUS.....	38

3.7 THE CYTOPLASMIC TAIL OF ERGIC-53 IS REQUIRED FOR BINDING TO UBXD1	40
3.8 UBXD1 INTERACTS WITH THE COPI β SUBUNIT	43
4. DISCUSSION.....	49
REFERENCES.....	57

LIST OF FIGURES

FIGURE	PAGE
FIG 1. COOMASSIE BRILLIANT BLUE STAINING OF PROTEINS FROM UBXD1 ^{FLAG} AND UBXD1 ^{FLAG} N184S IMMUNOPRECIPITATIONS.....	20
FIG. 2 VERIFICATION OF COOMASSIE BRILLIANT BLUE STAINING BY WESTERN BLOT.....	20
FIG. 3. PUB DOMAIN GENOTYPING RESULTS.....	22
FIG. 4. COOMASSIE BRILLIANT BLUE STAINING OF UBXD1 ^{FLAG} AND UBXD1 ^{FLAG} N184S IMMUNOPRECIPITATIONS SHOWING POTENTIAL N184S INTERACTING PROTEINS.....	25
FIG. 5. PONAESTERONE INDUCIBLE UBXD1 ^{FLAG} SYSTEM.....	33
FIG. 6. INDUCIBLE EXPRESSION OF UBXD1 ^{FLAG} FOLLOWED BY ANTI-FLAG IMMUNOPRECIPITATIONS SHOWS INTERACTION WITH ENDOGENOUS ERGIC-53.....	35
FIG. 7. SPECIFICITY OF ERGIC-53 BINDING AMONG p97 ADAPTOR PROTEINS.....	37
FIG. 8. UBXD1 N-TERMINUS IS REQUIRED FOR ERGIC-53 BINDING.....	39
FIG. 9. REQUIREMENT OF THE ERGIC-53 CYTOPLASMIC TAIL FOR INTERACTION WITH UBXD1.....	41
FIG. 10. ABILITY OF UBXD1 ^{FLAG} TO CO-IMMUNOPRECIPITATE COPI β SUBUNIT IN ADDITION TO ERGIC-53 AND p97.....	44
FIG. 11. MIRRORED PULLDOWN OF p97 AND β COP USING FLAG-TAGGED p97 ADAPTORS.....	46
FIG. 12. p97/ β COP INTERACTION IN THE PRESENCE AND ABSENCE OF UBXD1.....	47
FIG 13. MODEL FOR UBXD1 INTERACTION WITH β COP IN A p97 DEPENDENT MANNER.....	55

LIST OF TABLES

TABLE	PAGE
TABLE 1. PROTEIN MASS SPECTROSCOPY DATA FROM UBXD1 ^{FLAG} N184S IMMUNOPRECIPITATION.....	27
TABLE 2. RESULTS OF MudPIT ANALYSIS.....	31

LIST OF ABBREVIATIONS

- UBX** – Ubiquitin Regulatory X
- PUB** - Peptide:N-glycanase UBX-containing proteins
- VCP** – Valosin Containing Protein
- SNP** – Single Nucleotide Polymorphism
- ER** – Endoplasmic Reticulum
- ERAD** – ER-associated degradation
- UPS** – Ubiquitin-proteasome System
- PNGase** – Peptide: N-glycosidase
- p97^{UBXD1}** – p97 / UBXD1 complex
- UBXD1^{FLAG}** – C-terminal FLAG-tagged UBXD1
- UBXD1^{HA}** – C-terminal HA-tagged UBXD1
- ^{FLAG}ERGIC-53** – N-terminal FLAG-tagged ERGIC-53
- COP** – Coat Protein Complex
- ERGIC-53** – ER-Golgi intermediate compartment – 53
- IP** – Immunoprecipitation
- Co-IP** – Co-immunoprecipitation
- ERGIC** – ER-Golgi intermediate compartment
- F5F8D** – Combined Factor V-Factor VIII deficiency
- IBMPFD** – Inclusion Body Myopathy associated with Paget’s Disease of Bone and Frontotemporal Dementia
- ALS** – Amyotrophic Lateral Sclerosis
- UBXD1** – UBX domain containing protein 1

CHAPTER 1
INTRODUCTION

1.1 The AAA ATPase, p97 (VCP)

p97, also termed Cdc48 in yeast, is a member of the Type II AAA (ATPase Associated with Various Cellular Activities) ATPase Family of proteins. It is ubiquitously expressed within all eukaryotic cells, making up approximately 1% of total protein and is localized mainly within the cytosol, but can also be found associated with ER and Golgi membranes (Acharya et al., 1995; Latterich et al., 1995; Rabouille et al., 1995). p97 forms a homohexameric, two-tier barrel-shaped structure with a central pore that is occluded by a Zn^{2+} ion and can be broken down into six distinct domains; a N-terminus, N-D1 and D1-D2 linkers, D1 and D2 domains and a C-terminus.

AAA ATPase family members are known to oligomerize into a hexameric complex, which is believed to provide the mechanical basis for the characteristic ATPase activity essential to this family of proteins. Unlike other AAA ATPases, p97 does not require nucleotide binding for oligomerization. Instead, the D1 domain has been shown by both crystallography and biochemical studies to be the main domain involved in oligomerization of p97 (Wang et al., 2003a; Zhang et al., 2000b). In concert with these findings, it was later shown that the D1-D2 linker region also plays a pivotal role in nucleotide-independent hexamerization (Wang et al., 2003b). At present, however, exactly how this nucleotide independent oligomerization occurs is not fully understood.

The D2 domain is thought to be responsible for the major ATPase activity of p97, which is required for its function. However, within the literature there are discrepancies in the interpretation of whether or not the D2 domain acts alone in ATP hydrolysis or if it acts along with the D1 domain. Regardless of these incongruities, the ATPase domain contains Walker A and Walker B motifs that are thought to provide the nucleotide binding and hydrolysis activities. In addition to its ATPase activity, the D2 domain contains two loops that face toward the inner pore of the p97 hexamer. The first loop contains two arginine residues, Arg-586/Arg-589, important for ER-associated degradation (ERAD) activity and substrate-induced ATPase acceleration. In the ATP-bound state of the D2 domain, these residues face the inner pore and are thought to create a “denaturation collar” able to contribute to protein unfolding. The second loop contains a single tryptophan and phenylalanine residue, Trp-552/Phe-552, thought to create a hydrophobic patch able to interact with substrates (DeLaBarre et al., 2006).

Currently, there are two popular models that detail the interaction of p97 with its targeted substrates and how force is exerted on these substrates during this interaction. The first model proposed by DeLaBarre and Brunger suggests an interaction between the substrate and the “denaturation collar” to promote substrate unfolding while the variable helical D2 subdomains provide the force required to remove the target substrate from complexes. More specifically, force originates at the D2 ATPase domain while the D1 domain serves as the fulcrum to support the motion of the hexamer. The ATP bound state of the D2 domain transmits a conformational change through the D1-D2 linker to the N domain that is

bound to a substrate. Repeated cycles of ATP hydrolysis may provide the force to remove substrates from their associated complexes. In the second model, p97 is thought to act as a “molecular ratchet” such that both the D1 and D2 domains are capable of ATP hydrolysis. Through alternating their nucleotide-bound state, the domains move in an opposing manner. This movement is thought to provide the mechanical force that modifies the substrate protein’s conformation, allowing it to be segregated from a complex (Zhang et al., 2000).

The C-terminal tail of p97 contains a major tyrosine phosphorylation site, Tyr-805. Phosphorylation of the tyrosine residue appears to play a role in growth and differentiation related functions (Egerton et al., 1992, Ficarro et al., 2003), but how it functions within these pathways remains largely unknown. It has also been shown that phosphorylation of the C-terminus does not alter the ATPase activity of p97 (Egerton and Samelson, 1994). Speculations based on this and other data suggest phosphorylation may serve as a localization signal or regulate association of p97 with different adaptors or target proteins (Wang et al., 2004).

The p97 N-terminus is responsible for binding various co-factors, otherwise known as adaptor proteins (Dai and Li, 2001). While it is not required for hexamerization or ATPase activity, cryo-EM studies have suggested that the spatial orientation of the amino-terminal tail is affected by the nucleotide bound state of the D2 domain (Rouiller et al., 2002). When the D2 domain is bound by ATP, the D1-D2 linker relays the conformational information to the D1 helical subdomain to restrict the N domain to a fixed position. When in the ADP-bound state, the

conformation change in the D1-D2 linker frees the N-terminal tail, allowing it to participate in adaptor binding (Beuron et al., 2003; Zhang et al., 2000b).

p97 mediates a wide variety of cellular processes ranging from participation of p97 in ERAD when bound by the Ufd1-Npl4 adaptor complex, to Golgi regrowth and membrane fusion when bound by the trimeric p47 adaptor. Most notably, p97 plays an essential role in protein degradation via the ubiquitin-proteasome system (UPS). The importance of p97 within the UPS can be observed upon loss of p97 function leading to a build-up of ubiquitinated proteins within the cell (Wojcik et al., 2004), a consequence that is shared by various proteinopathies. In particular, IBMPFD and very recently ALS have been shown to display this cellular phenotype. Currently, the molecular basis for these pathologies is unknown. Originally, it was thought that disease-associated mutations within p97 impaired ubiquitin-dependent proteasome degradation by the proteasome. However, recent data suggests this is not the case. Instead, it has been proposed that these mutations impair autophagosome maturation, which is a crucial early step in the autophagy pathway. To this point, it was shown that expression of an IBMPFD-associated p97 mutant led to accumulation of large, ubiquitin-positive “rimmed vacuoles” in addition to accumulation of LAMP-I/LAMP-II and LC3-II protein indicative of a defect in autophagy (Tresse et al, 2010). This evidence makes a strong argument that p97 is required for proper maturation of autophagosomes for proper autophagy to take place. While the adaptors that mediate p97 function in this process are currently unknown, mutations occurring within the N-terminus, N-D1

linker and D1 domain of p97 may affect the ability of p97 to interact with adaptors, consequently affecting proper p97 function within the autophagy pathway.

1.2 The 'Ubiquitin Regulatory X' (UBX) Domain

The subcellular localization and function of p97 is controlled by adaptor proteins, which bind p97 through various domains. The UBX domain containing family of adaptors is the largest family of *bona fide* p97 adaptor proteins. The approximately 80 amino-acid UBX domain was originally identified in human SAKS1 as having weak sequence homology to ubiquitin. Subsequent structure-based studies revealed that the UBX domain adopts the same three-dimensional fold as ubiquitin however it lacks the C-terminal di-glycine motif for interaction with target substrates and crucial lysine residues involved in ubiquitin conjugation and chain formation (Buchberger et al., 2001). Thus, while the UBX domain is structurally similar to ubiquitin making it conceivable that it could participate in ubiquitin-mediated activities such as the UPS, lack of these residues make it highly unlikely to participate in such processes. Structure-based sequence alignment of UBX domains revealed a highly conserved surface patch consisting of an arginine residue in strand 1 and a phenylalanine, proline, arginine motif in the loop connecting strands 3 and 4 (Buchberger et al., 2001). This conserved surface patch was then shown to bind a hydrophobic pocket between the two subdomains of the p97 N-domain (Dreveny et al., 2004).

1.3 The Peptide:N-glycanase UBX-containing proteins (PUB) Domain

In addition to the UBX domain containing family of adaptors, proteins containing a PUB (Peptide:N-glycanase UBX-containing proteins) domain have been implicated in binding to p97. The PUB domain was originally discovered in homologues of the PNG1 gene encoding the peptide: N-glycanase (PNGase) enzyme. The cytoplasmic PNGase is a deglycosylating enzyme thought to participate in proteasome-dependent degradation of misfolded glycoproteins that are translocated from ER to cytosol (Suzuki, 1997). Shortly after the discovery of the PNG1 gene, homologues of the gene product (Png1p) were found in higher eukaryotes. Interestingly, these homologues contained N- and C-terminal extensions. A group interested in finding homologues of Pngp1 in the plant, *Arabidopsis thaliana*, found proteins having significant homology to the extended N domain of Png1p. Further analysis of these proteins revealed some to also contain a UBX domain. The region was therefore named Peptide:N-glycanase UBX-containing proteins, or PUB (Suzuki et al., 2001). Using human PNGase, the PUB domain was found to interact with p97 via an evolutionarily conserved surface patch consisting of an asparagine, lysine and tyrosine residue (Allen et al., 2006).

1.4 UBXD1

After the discovery of the interaction between the PUB domain and p97, a yeast two-hybrid screen of a HeLa cell cDNA library using p97 as bait revealed UBXD1 as a novel p97 interacting protein. Subsequent analysis revealed UBXD1 to contain two known p97 interaction modules; a central PUB domain and a C-terminal

UBX domain (Madsen et al., 2008). Interestingly, the UBX domain of UBXD1 lacks the conserved FPR motif that is required to mediate binding to p97 (Dreveny et al., 2004). However, it has been shown by both *in vitro* and *in vivo* analysis that both the PUB and N-terminal domain of UBXD1 preferentially interact with p97 (Allen et al., 2006; Zhao et al., 2007; Madsen et al., 2008; Kern et al., 2009). Association of the PUB domain occurs at the C-terminus of p97 and is stabilized by hydrophobic and ionic forces upon insertion of the C-terminal Tyr805 residue into a hydrophobic pocket within the PUB domain itself (Zhao, 2007). Studies have shown phosphorylation of the penultimate tyrosine residue abolishes PUB domain binding (Zhao et al., 2007; Madsen et al., 2008), however future studies are required to determine the role PUB domain binding plays in the absence of p97 C-terminal tail phosphorylation. In addition to the PUB domain, a highly conserved region within the first 150 amino acids of the UBXD1 N-terminus has been shown to participate in p97 binding (Kern et al., 2009). While this interaction data sheds light on UBXD1 domains required for p97 binding, the cellular function of UBXD1 remains largely unknown.

1.5 ERGIC-53

ER-Golgi Intermediate Compartment-53 (ERGIC-53) is a nonglycosylated, type-I single span membrane protein that serves as a marker for the ERGIC (ER-Golgi), as it is mostly concentrated at this location within the cell. ERGIC-53 consists of 510 amino acids that include an N-terminal signal sequence of 30 residues, a carbohydrate recognition domain of 240 residues, a stalk region of 210 residues, a trans-membrane domain of 18 residues and a 12 amino acid cytoplasmic tail. The C-

terminal tail of ERGIC-53 plays an important role in the localization and trafficking of the protein. ERGIC-53 has been shown to cycle between the ER, ERGIC and cis-Golgi to transport a specific group of glycoprotein cargo. The last four amino acids of the C-terminus consist of two lysine residues(KK) and two phenylalanine residues(FF), which as a whole form a KKFF motif. The phenylalanine residues are required for binding Coatamer Protein Complex II (COPII) for trafficking of ERGIC-53 and bound client proteins to the ERGIC for further sorting (Kappeler et al., 1997). The lysine residues are required for binding Coatamer Protein Complex I (COPI) for proper recycling of ERGIC-53 from the ERGIC back to the ER. ERGIC-53 binding to clients can occur independently or through binding to its co-factor, Multiple Coagulation Factor Deficiency 2 (MCFD2). Mutations within both ERGIC-53 and MCFD2 have been linked to the coagulation disorder Combined deficiency of factor V and factor VIII (F5F8D), leading to decreased plasma levels of coagulation factors V and VIII (Nichols et al., 1999). Recent studies within our lab have shown a novel interaction between an N-terminal domain of UBXD1 and the C-terminal tail of ERGIC-53, but the functional significance of this interaction is yet to be determined.

1.6 Research Focus, Hypothesis and Goals

One focus of the Haines laboratory is to elucidate the function of UBXD1. Unpublished results from within the laboratory suggest UBXD1 to be defective at interacting with p97 mutants found in IBMPFD and ALS disease, leading to a disruption of the autophagy pathway. Consistent with this, preliminary studies indicate shRNA-mediated depletion of UBXD1 suppresses autophagy. These results suggest a role for UBXD1 as a human disease relevant protein. Variations within the

DNA sequence caused by SNPs can determine an individual's susceptibility to disease in addition to their responsiveness to various therapies. Within the past decade, there has been a strong interest in using personalized medicine in the treatment of diseases associated with various SNPs. Search of a SNP database for polymorphisms within conserved regions of UBXD1 was carried out. Interestingly, the SNP database revealed a polymorphic variant that contained a polymorphism within a conserved region of the PUB domain. The SNP was found within the asparagine residue of the evolutionarily conserved surface patch, resulting in an asparagine(N) to serine(S) substitution, termed N184S.

The two main objectives of my master's thesis project have been 1) to characterize this UBXD1 polymorphic variant in terms of p97 binding capabilities and determine the prevalence of the N184S PUB domain SNP within the population and 2) identification/verification of UBXD1 interacting proteins that may provide a clue for UBXD1 function in autophagy and define domains required for association.

Based on preliminary data within the lab, my hypothesis is that the UBXD1 N-terminus is required for binding to ERGIC-53 and that the cytoplasmic tail of ERGIC-53 is required for UBXD1 binding given that UBXD1 exists as a peripheral membrane-associated protein. If a p97UBXD1 complex is indeed interacting with ERGIC-53, this interaction may lead to further interactions that will assist in determining the cellular function of UBXD1.

CHAPTER 2
MATERIALS AND METHODS

2.1 Plasmid Preparation

2.1.1 UBXD1^{FLAG} N184S

The coding sequence of full-length human UBXD1 had been previously cloned into a pCEP vector and was available for use within the laboratory. A mutation resulting in a single amino-acid change in the UBXD1 PUB domain (N184S) was introduced by PCR site-directed mutagenesis using the primers 5'-TTGCCAAGTACCTAGACAGCATCCACCTGCAC-3' and 3'-AACGGTTCATGGATCTGTCGTAGGTGGACGTG-5' (Sigma). The primers were designed to introduce a Pst-1 restriction site for screening purposes. PCR site-directed mutagenesis was carried out using an online protocol referencing methods used by Zheng et al., 2004. After PCR, the reaction product was tested using the Pst-1 restriction site followed by Dpn1 digestion and transformation in XL-2 Blue Competent cells(Stratagene). Cells were plated on LB agar plates containing ampicillin and placed at 37°C overnight. Colonies were picked and cultured in LB containing ampicillin at 37°C overnight. DNA was purified using Qiagen Mini-Prep and sent out for sequencing.

2.1.2 FLAG-ERGIC-53

The coding sequence of full length human LMAN1 (ERGIC-53) was obtained in a pCMV-Sport6 vector from Open BioSystems. PCR site-directed mutagenesis was used to place a N-terminal FLAG tag on full length ERGIC-53 downstream of the N-terminal signal sequence cleavage site using the primers 5'-

TCACTCGGTTCGCTTCGTCCGGGGCGACTACAAGGATGACGACGATAAGGGCGGAGGAGAC
CCCGCGGTCGCG-3' AND 3'-

AGTGAGCCAGCGAAGCAGGCCCGCTGATGTTCTACTGCTGCTATTCCCGCACCCCTCCTC
TGGGGCGCCAGCGC-5' (Sigma). The primer was designed to introduce a SacII

restriction site for screening purposes. PCR site-directed mutagenesis was carried out using an online protocol referencing methods used by Zheng et al., 2004. After PCR, the reaction product was tested using the SacII restriction site followed by Dpn1 digestion and transformation in XL-2 Blue Competent cells(Stratagene). Cells were plated on LB agar plates containing ampicillin and placed at 37°C overnight. Colonies were picked and cultured in LB containing ampicillin at 37°C overnight. DNA was purified using Qiagen Mini-Prep and sent out for sequencing.

2.2 Tissue Culture

2.2.1 H1299 and 293T cells

H1299 and 293T cells were cultured in 10cm dishes and maintained in complete media (DMEM(Cellgro) supplemented with 10% FBS and 10,000 I.U./ml penicillin, 10,000 µg/ml streptomycin) at 37C in 5% CO₂.

2.2.2 pIND cell line

An inducible cell line was generated in the H1299 cell line to express UBXD1^{FLAG} upon treatment with ponasterone. Cells were maintained in DMEM(Cellgro) supplemented with 10% FBS and 400 µg/ml zeomycin, .5ug/ml puromycin and 200 µg/ml neomycin.

2.2.3 miR30-based cell system

A cell line was generated in H1299 cells to produce shRNA against UBXD1 upon treatment with doxycycline. Cells were maintained in DMEM(Cellgro) supplemented with 10% FBS and 100 µg/ml hygromycin.

2.3 Transfections

2.3.1 H1299 cells

H1299 cells were seeded to an approximate confluence of 40% in 10cm tissue culture plates(Denville). Approximately one hour prior to transfection, the media from the plates was removed and 10ml fresh complete media (DMEM(Cellgro) supplemented with 10% FBS and 10,000 I.U./ml penicillin, 10,000 ug/ml streptomycin) was added. DNAs were prepared and brought to a final concentration of 3 µg with appropriate vector-alone plasmid DNA. A total of 3 µg of DNA was added to a polystyrene tube containing 488ul DMEM and 12µl fugene(Roche). After 30-40 minutes of incubation at ambient temperature of DNA

in the presence of fugene, the mixture was added dropwise to the appropriate plate and incubated at 37°C for 48 hours.

2.3.2 293T cells

293T cells were seeded to an approximate confluence of 80% in 10cm tissue culture plates(Denville). Approximately one hour prior to transfection, the media from the plates was removed and 10ml fresh complete media (DMEM(Cellgro) supplemented with 10% FBS and 10,000 I.U./ml penicillin, 10,000 µg/ml streptomycin) was added. DNAs were prepared and brought to a final concentration of 3 µg with appropriate vector-alone plamid DNA. A total of 3µg of DNA was added to a polystyrene tube containing 488ul DMEM and 12µl fugene(Roche). After 30-40 minutes of incubation at ambient temperature of DNA in the presence of fugene, the mixture was added dropwise to the appropriate plate and incubated at 37°C for 48 hours.

2.4 Immunoprecipitations

2.4.1 FLAG Immunoprecipitations(IP RIPA)

Cells were harvested and lysed with ice-cold IP RIPA lysis buffer (50mM Tris pH 7.4, 1mM EDTA pH 8.0, 150mM NaCl, 1% NP-40, .25% deoxycholate acid with 1mg/ml Pepstatin A, 1mg/ml Aprotinin, 1mg/ml Trypsin Inhibitor, .0174mg/ml PMSF). Protein levels were quantified via Bradford Reagent(BioRad) and normalized to a final concentration of 3 µg/µl with RIPA lysis buffer. A total of 20µl

of cell lysate was taken for input samples and 5ul of 4x SDS-loading dye was added. 600µg of protein was pre-cleared using 20ul of 25% IgG agarose(Sigma) beads for 2 hours on the inversion wheel. After 2 hours, samples were briefly centrifuged at room temperature and the supernatant was transferred to a separate eppendorf tube. A volume of 20µl of 50% anti-FLAG M2 agarose beads(Sigma) was added and tubes were put on the inversion wheel overnight in the cold room. The following day, samples were centrifuged at room temperature and washed 3 times in 500µl of IP RIPA buffer. Following washing, beads were re-suspended in 40µl of 1x SDS-loading dye and boiled in preparation for western blot.

2.4.2 FLAG Immunoprecipitations (EBC)

Cells were harvested and lysed with ice-cold EBC lysis buffer(50mM Tris-HCl pH 7.5, 120mM NaCl, 1% NP-40). Protein levels were quantified via Bradford Reagent(BioRad) and normalized to a final concentration of 3 µg/µl with EBC lysis buffer. A total of 30µl of lysate was taken for input samples and 10µl of 4x SDS-loading dye was added. 1 mg of protein was used for immunoprecipitations and 25µl of 50% anti-FLAG M2 agarose beads(Sigma) were added. Samples were then placed on the inversion wheel for 3 hours. After time elapsed, samples were briefly centrifuged and washed 4 times with 500µl of EBC lysis buffer. After the final wash, beads were re-suspended in 50µl of 1x SDS-loading dye and boiled in preparation for western blot.

2.4.3 HA Immunoprecipitations

Cells were harvested and lysed with ice-cold EBC lysis buffer (50mM Tris-HCl pH 7.5, 120mM NaCl, 1% NP-40). Protein levels were quantified via Bradford Reagent (BioRad) and normalized to a final concentration of 3 µg/µl with EBC lysis buffer. A total of 30ul of lysate was taken for input samples and 10µl of 4x SDS-loading dye was added. 1 mg of protein was used for immunoprecipitations and 25µl of 50% anti-HA agarose beads (Sigma) were added. Samples were then placed on the inversion wheel for 3 hours. After time elapsed, samples were briefly centrifuged and washed 4 times with 500µl of EBC lysis buffer. After the final wash, beads were re-suspended in 50µl of 1x SDS-loading dye and boiled in preparation for western blot.

2.5 Western Blotting

A total of 30µg of sample input and 10µg of immunoprecipitated protein were loaded onto a 7.5% acrylamide gel. Proteins were resolved by SDS-PAGE in running buffer and transferred to a nitrocellulose membrane(GE Healthcare) in transfer buffer for 1 hour. After transfer, membranes were stained with Ponceau S stain(Sigma) to assess loading and then briefly washed with PBS-T buffer until ponceau dye washed off. Membranes were then blocked in 5% milk solution(BioRad) for one hour. The membranes were then probed with the appropriate antibody overnight 4°C. The following day, membranes were washed a total of three times for ten minutes each at room temperature with PBS-T buffer. After washing, membranes were probed with the appropriate secondary anti-body

for one hour then washed a total of three times for ten minutes each at room temperature with PBS-T. After the final wash, Western Lighting Plus ECL reagent(PerkinElmer) was then added to the membrane and the resultant bands were recorded on blue X-Ray film(Phoenix).

2.6 Protein Gel Fixing and Staining with Coomassie Brilliant Blue

Immunoprecipitated proteins were resolved by SDS-PAGE. Proteins were then fixed by placing the gel in fixing solution(40% methanol, 10% acetic acid in water) on the shaker for 15 minutes. The gel was then stained with Coomassie Brilliant Blue(BioRad) for 30 minutes and destained with fixing solution until deemed sufficient. Gels were then placed on filter paper and dried using a gel dryer(BioRad).

2.7 Genotyping of the UBXD1 PUB domain

PCR was used to genotype the PUB domain of human genomic DNA using the primers 5'-ACCTGAAACACCTTGTCTGC-3' and 3'-GTGTGAACCGGAGATCAGTCT-5'. Template DNA was used at concentration of 10ng/ μ l. PCR reaction was purified using a DNA Clean and Concentrator Kit (Zymo Research). Purified samples were then sent out to be sequenced.

2.8 Ponasterone Inducible System

To induce expression of UBXD1^{FLAG} in the inducible cell line, cells were seeded to approximately 50% confluency then treated with .1 μ M, .3 μ M, 1 μ M or 3 μ M

of ponasterone in DMEM(Cellgro) supplemented with 10% FBS and 400µg/ml zeomycin, .5µg/ml puromycin and 200µg/ml neomycin. After 24 hours, old media was removed and new ponasterone containing media was applied to cells at the appropriate concentration. After a total of 48 hours of treatment with ponasterone, cells were harvested.

2.9 UBXD1 Knock-down

To induce knockdown of UBXD1 within the miR30-based system, cells were split and seeded to a confluency of approximately 50% in DMEM(Cellgro) supplemented with 10% FBS and 100 µg/ml hygromycin. Cells were then treated with media containing doxycycline at a concentration of 2 µg/ml. Every 24 hours, for 96 hours, old media was removed and new media containing doxycycline was added.

CHAPTER 3

RESULTS

3.1 Loss of Binding phenotype with UBXD1 Polymorphic Variant, UBXD1

N184S

As discussed previously, the UBXD1 PUB domain has been shown to bind to the C-terminal tail of p97. While a search of a SNP database revealed multiple SNPs outside of conserved regions of the protein, one was found to occur within the PUB domain resulting in an asparagine to serine amino acid change. This SNP was originally catalogued as a result of the Japanese Millennium Genome Project (Haga et al., 2002). Subsequently, a structure based sequence alignment of PUB domains across six distantly related eukaryotic species revealed the asparagine residue (Asn-41) to be absolutely conserved among them. In cooperation with two other highly conserved lysine (Lys-50) and tyrosine (Tyr-51) residues, asparagine lines a basic pocket on the surface of UBXD1 (Allen and Bycroft, 2006). It has been suggested that the clustering of these three highly conserved amino acids constitutes a functionally important site by forming a hydrophobic pocket required for p97 binding. Given this information, I hypothesized that a SNP at the absolutely conserved asparagine residue within the PUB domain of UBXD1 affects its ability to interact with p97. Considering recent data within our laboratory suggesting p97^{UBXD1} to be involved in degradation of misfolded proteins within the autophagy pathway (data not shown), such an altered cellular phenotype could have disease relevant consequences.

In order to assess the ability of the UBXD1 polymorphic variant to bind p97, I generated a construct for use in immunoprecipitation experiments. A C-terminal flag-tagged UBXD1 construct(UBXD1^{FLAG}) in a pCEP vector had been previously generated and available for use within our laboratory. Using PCR site-directed mutagenesis with primers designed to mutate Asn-41 into a serine residue, I was able to produce a C-terminal FLAG-tagged construct containing this polymorphism, called UBXD1^{FLAG} N184S. To test my hypothesis, I transfected H1299 cells with increasing amounts of full-length UBXD1^{FLAG} or UBXD1^{FLAG} N184S construct. After 48-hours, cells were harvested, lysed in RIPA buffer, protein quantified and lysate prepared to a final concentration of 3 µg/µl. Immunoprecipitations were carried out using anti-FLAG antibody conjugated beads. Samples were then resolved by SDS-PAGE and the gel was fixed and stained with Coomassie Brilliant Blue. Figure 1 demonstrates UBXD1^{FLAG} interaction with endogenous p97 as being relative to the amount of UBXD1^{FLAG} transfected into cells and that this effect was significantly reduced in the UBXD1^{FLAG} N184S immunoprecipitation.

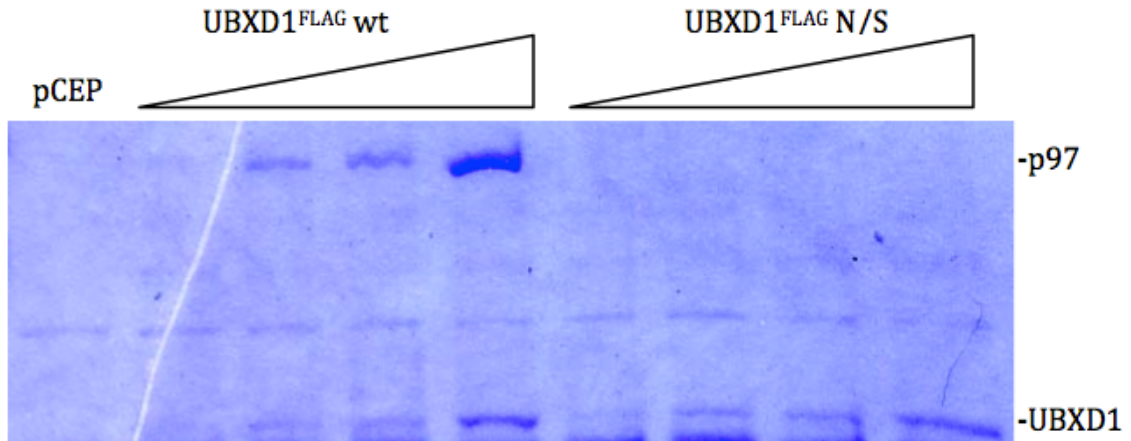


Figure 1. Coomassie Brilliant Blue staining of proteins from UBXD1^{FLAG} and UBXD1^{FLAG} N184S immunoprecipitations. H1299 cells were transfected with an increasing amount (.375 μ g, .75 μ g, 1.5 μ g, 3 μ g) of UBXD1^{FLAG} or UBXD1^{FLAG} N184S. Immunoprecipitations were carried out using anti-FLAG antibody conjugated beads and proteins were resolved by SDS-PAGE. The gel was then fixed and stained with Coomassie Brilliant Blue.

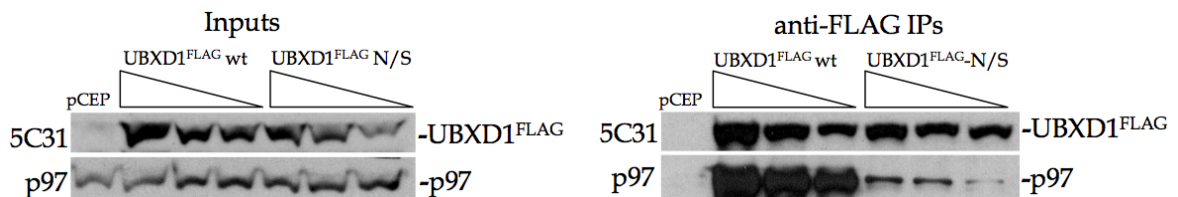


Figure 2. Verification of Coomassie Brilliant Blue staining by western blot. Immunoprecipitated samples from the previous experiment (excluding the 3 μ g sample) were resolved by SDS-PAGE, transferred onto nitrocellulose membrane and probed using anti-p97 or anti-UBXD1 antibodies.

To confirm these results, I performed a western blot using the same samples as were previously used. Immunoprecipitated samples were resolved by SDS-PAGE, transferred onto nitrocellulose membrane and probed using anti-p97 or anti-UBXD1 antibodies. The results shown in Figure 2 reveal a robust interaction between full-length UBXD1^{FLAG} and endogenous p97 relative to the amount of construct transfected into cells while the ability of UBXD1^{FLAG} N184S to bind endogenous p97 was drastically reduced, thus confirming the results observed by Coomassie staining.

Based on the Coomassie Brilliant Blue staining and western blot analysis, I concluded that the UBXD1 N184S polymorphic variant displayed a decreased ability to bind endogenous p97 compared to transfected full-length UBXD1^{FLAG} in H1299 cells under our conditions. This result was likely due to mutation of one of the three amino acids (Asn-184) that lines a basic pocket on the surface of UBXD1 thought to be required for p97 binding. As stated previously, adaptor binding plays an important role in the cellular function of p97. Thus, expression of this polymorphic variant may cause a defect in “p97^{UBXD1} complex dependent activities” contributing to a cellular disease phenotype. To further examine this hypothesis, I sought to verify the prevalence of the UBXD1 PUB domain N184S SNP within the population.

3.2 Determining the Frequency of the UBXD1 N184S Polymorphism

We obtained thirty-six placental DNA samples from presumably genotypically and phenotypically normal mother and fetus that had been previously prepared and purified. Samples were then diluted to a final concentration of 10 ng/ μ l for use as template DNA in the PCR reaction. Primers were designed to obtain proper amplification of the PUB domain. After PCR, samples were run out on a 2% agarose gel to determine efficiency of amplification, excised from the agarose gel and purified using the Zymo Research DNA Clean and Concentrator Kit, then run out again on a 2% agarose gel to determine concentration. Samples were sent out for sequencing using our 3' UBXD1 primer. Results from the sequencing revealed all thirty-six samples tested to have a wild-type PUB domain (Figure 3).

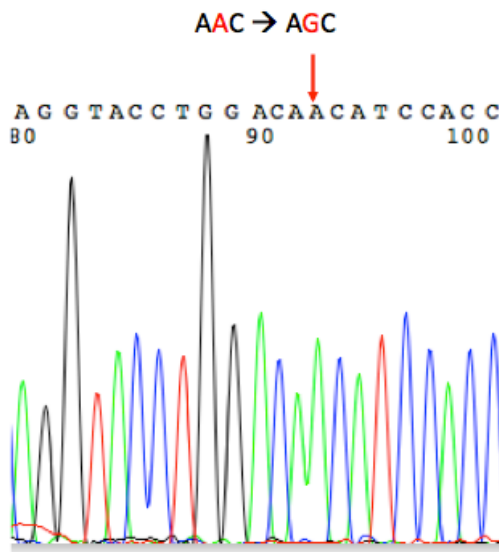


Figure 3. PUB Domain Genotyping Results. Results of the sequencing of human PUB domain in an attempt to verify the UBXD1 N184S SNP.

In other words, none of the samples tested contained the N184S mutation within the PUB domain. Since the N184S PUB domain SNP was originally found to be present using DNA from a person of Japanese descent, I decided to repeat the experiment using only DNA samples from people of Asian descent. A total of sixteen Asian DNA samples were acquired. Methods for the PCR, purification and sequencing were performed in the same manner as before. However, the sequencing results again failed to confirm the presence of the N184S SNP within the sixteen Asian DNA samples tested.

3.3 Attempting to Identify UBXD1 N184S Interacting Proteins by a Mass Spectroscopy Proteomics Approach

Regardless of our ability to verify the N184S SNP, the interaction data showed a severe loss in p97 binding. Looking back on these data, I observed a potentially interesting result. Using the UBXD1^{FLAG} N184S mutant, I visualized bands that were otherwise obscured by the prevalence of p97 binding to the full-length UBXD1^{FLAG} construct and set out to identify these potential UBXD1 interacting proteins.

H1299 cells were transfected with either UBXD1^{FLAG} wt (3 μ g) or UBXD1^{FLAG} N184S (3 μ g). Samples were harvested 48 hours post-transfection and prepared as previously stated. Immunoprecipitations were performed using anti-FLAG antibody conjugated beads. Samples were then resolved by SDS-PAGE. The gel was then fixed and stained with Coomassie Brilliant Blue. Samples run on a 10% acrylamide gel using SDS-PAGE revealed the potential UBXD1 N184S interacting proteins around 95-100 kDa and 100-120 kDa that were seemingly not present in the control or the UBXD1^{FLAG} wt immunoprecipitations (Figure 4). The bands were excised from the acrylamide gel and sent out to be analyzed by mass spectroscopy.

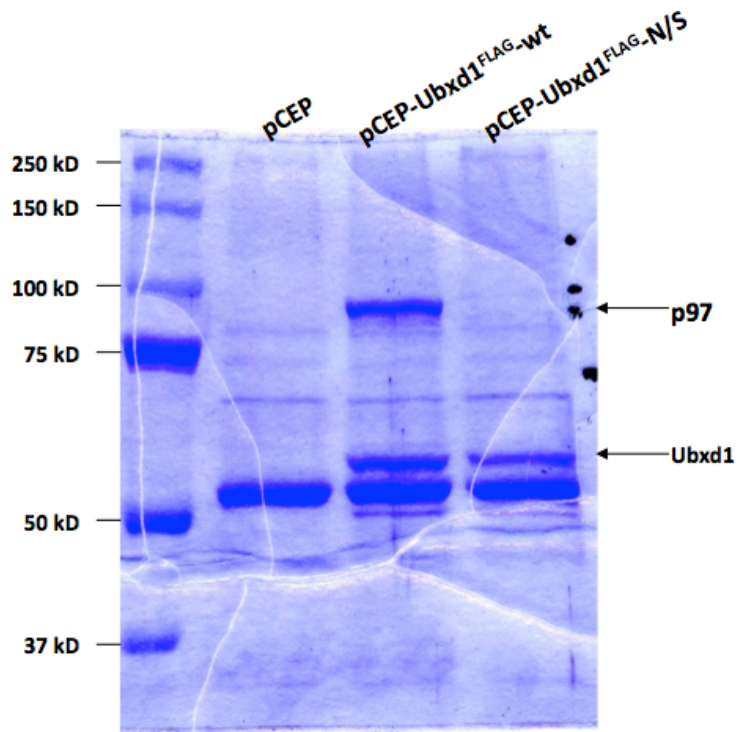


Figure 4. Coomassie Brilliant Blue staining of UBXD1^{FLAG} and UBXD1^{FLAG} N184S Immunoprecipitations showing potential UBXD1 N184S interacting proteins. H1299 cells were transfected with 3 μ g of UBXD1^{FLAG} or 3 μ g of UBXD1^{FLAG} N184S. Immunoprecipitations were performed using anti-FLAG antibody conjugated beads then proteins were resolved by SDS-PAGE. The gel was then fixed and stained with Coomassie Brilliant Blue.

Mass spectroscopy data from the higher molecular weight band yielded essentially no useful insight into potential UBXD1 interacting proteins. The highest number of spectral hits was a proteasome subunit, which could simply be due to the fact that UBXD1 is a ubiquitin modified protein. The results from the lower molecular weight band revealed p97 as the protein with the highest number of spectral hits (Table 1). This result was not particularly surprising as the result from our immunoprecipitation failed to show a complete loss of p97 binding but rather a severely decreased ability in UBXD1^{FLAG} N184S to bind p97. Thus, a low level of residual p97 was present. In addition to p97, various other proteins were identified

Gene Name	NCBI Accession Number	Number of Assigned Spectral Hits (Band 1)	Number of Assigned Spectral Hits (Band 2)
VCP	IPI00022774	41	0
PSMD2	IPI00012268	11	2
OGT Isoform 3	IPI00005780	0	10
MTHFD1	IPI00218342	0	9
HSPA4	IPI00002966	0	8
EEF2	IPI00186290	7	0
NSUN2	IPI00306369	0	6
IPO8	IPI00007401	3	7
MCM4	IPI00018349	5	3
HSPH1	IPI00218993	0	6
MSH2	IPI00017303	0	5
E2F7	IPI00414604	0	5
MMS19	IPI00154451	0	4

Table 1. Protein Mass Spectroscopy Data from UBXD1^{FLAG} N184S

Immunoprecipitation. H1299 cells were transfected with either UBXD1^{FLAG} wt(3µg) or UBXD1^{FLAG} N184S(3µg). Samples were harvested 48 hours post-transfection and prepared as previously stated. Immunoprecipitations were performed using anti-FLAG antibody conjugated beads. Samples were then resolved by SDS-PAGE. The gel was then fixed and stained with Coomassie Brilliant Blue. Samples run on a 10% acrylamide gel using SDS-PAGE revealed the potential UBXD1 N/S interacting proteins around 95-100 kDa and 100-120 kDa that were seemingly not present in the control or the UBXD1^{FLAG} wt immunoprecipitations. The bands of interest were excised from the acrylamide gel and sent out to be analyzed by mass spectroscopy. Results of the mass spectroscopy proteomics are presented in the table.

including PSMD2, a non-ATPase subunit of the 19S proteasome lid, OGT a glycosyltransferase, MTHFD1 an enzyme that catalyzes de novo purine synthesis, HSPA4 a heat shock protein, as well as many others. However, none of the proteins showed a strong enough interaction with the UBXD1 polymorphic variant to justify further verification.

During the course of these studies, a unique opportunity to identify UBXD1 interactions using more sophisticated MudPIT (Multidimensional Protein Identification Technology) analysis presented itself to Dr. Haines. As a result, he spent three months in the laboratory of Dr. Raymond Deshaies at the California Institute of Technology using this technology to identify novel UBXD1 interacting proteins. My further UBXD1 interaction studies were placed on hold, pending Dr. Haines' results.

3.4 Solution Based Proteomics Reveals a Novel UBXD1 Interacting Protein, ERGIC53

MudPIT analysis gives many advantages over the previous approach due to the nature of how samples are prepared and analyzed. The protein sample is first digested into its constituent peptides, which are then separated with two liquid column chromatography steps. The first step is a strong cationic exchange followed by the second step of reversed-phase high performance liquid chromatography. As the peptides elute from the second column, they are sprayed into a linear ion trap mass spectrometer. The first MS scan assigns each peptide a mass/charge ratio. The most intense peptide signals are then fragmented in a second MS/MS scan, which assigns each peptide a unique “fingerprint.” The fingerprints are then fed into bioinformatics databases that reveal the protein’s identity (Netterwald, 2007).

Three separate immunoprecipitation experiments were performed using a c-terminal FLAG-tagged UBXD1 construct. Two of these used a ponasterone-inducible system to express the UBXD1^{FLAG} construct, while the other involved transient transfection of 293T cells with UBXD1^{FLAG}. In the two separate inducible system experiments, cells were treated with either .1 μ M or .3 μ M ponasterone for 48 hours. Cells were then harvested, lysed and lysate normalized to 3 μ g/ml. A total of 1mg of protein was used for the immunoprecipitation with anti-FLAG antibody conjugated beads. After washing, proteins were eluted from beads with 10M urea. The eluent was reduced with TCEB and subjected to a four-hour Lyse C digestion and a fourteen-hour trypsin digestion. The samples were desalted, lyophilized and resuspended in 0.2% formic acid. Samples were then subjected to MudPIT analysis.

The results from the MudPIT analysis can be found in Tables 2a-c. This summary does not include proteins whose peptides were found in control anti-FLAG immunoprecipitations from empty vector transfected (293T) or ponasterone (H1299) treated cells nor does it include peptides present less than 5 spectral hits in anti-FLAG immunoprecipitation derived from cells expressing UBXD1^{FLAG}.

In addition to the presence of expected p97 and UBXD1, peptides of the mannose-binding ER resident protein, ERGIC-53, were also identified in a significant number of spectral hits in each experiment. ERGIC-53 is a nonglycosylated type-I single spanning trans-membrane protein that is localized to the ER-Golgi intermediate compartment (ERGIC) where it serves as a transporter of glycoprotein clients between the ER, ERGIC and cis-Golgi in the early secretory pathway. Present as a hexamer, ERGIC-53 contains a short cytoplasmic tail domain containing a C-terminal KKFF motif required for proper targeting of the protein within the ER-ERGIC-Golgi pathway, a trans-membrane domain, a stalk region containing two cysteines required for oligomerization, a carbohydrate recognition domain required for interaction with its client proteins and an amino terminal region. The process of client transport and ERGIC-53 recycling occurs through the following general steps. Newly synthesized ERGIC-53 monomers translocate to the lumen of the rough ER and oligomerize to form homohexameric ERGIC-53 capable of binding clients. Upon complex formation with a client, ERGIC-53 is recruited by COPII vesicles leading to budding from the ER membrane and subsequent client release in the ERGIC. Upon release, ERGIC-53 recycles back to ER via COPI vesicles. It is thought that client binding and transport acts as a secondary protein quality-control step for ERGIC-53

a.

Gene symbol or name	NCBI Accession #	# of assigned spectra
P97	IPI00022774	179
UBXD1	IPI00019276	60
ERGIC-53	IPI00026530	22
RPS5	IPI00008433	9
LIMAI	IPI00008918	6
HNRNPK	IPI00216049	6
TJP1	IPI00216219	5

b.

Gene symbol or name	NCBI Accession #	# of assigned spectra
P97	IPI00022774	440
UBXD1	IPI00019276	94
ERGIC-53	IPI00026530	25
LIMAI	IPI00008918	16
GAPDH	IPI00219018	14
MYO6	IPI00008455	12
MYO18A	IP00334410	10
CLTC	IPI00024067	10
UBB	IPI00179330	8
SEPT9	IPI0078614	8
PDLIM7	IPI00023122	7
TPM1	IPI00216134	7
RPLP1	IPI00008527	7
HSPA8	IPI00003865	7
RPS5	IPI00008433	6
DBN1	IPI00003406	6
SRGAP2	IPI00479125	6
Nucleolin	IPI00444262	5
RPL23	IPI00010153	5
CAV1	IPI00009236	5
SRP14	IPI00293434	5
RPS10	IPI00008438	5

c.

Gene symbol or name	NCBI Accession #	# of assigned spectra
P97	IPI00022774	1151
UBXD1	IPI00019276	685
ERGIC-53	IPI00026530	126
ASPSCR1	IPI00065276	10
MCFD2	IPI00328680	8
UBB	IPI00179330	7

Tables 2a-c. Results of MudPIT analysis. In

Table 2a, cells were treated with .1uM ponasterone, leading to expression of UBXD1^{FLAG} at near

physiologic levels of UBXD1. In Table 2b, cells were treated with 3uM ponasterone leading to an approximate 30-fold over-expression of UBXD1^{FLAG}.

In Table 2c, 293T cells were transiently transfected UBXD1^{FLAG}.

This summary of results does not include proteins whose peptides were found in control anti-FLAG immunoprecipitations nor does it include peptides present less than 5 spectral

hits in anti-FLAG immunoprecipitation derived from cells expressing UBXD1^{FLAG}.

client glycoproteins upon exiting the ER. In this model, only properly folded clients will be recognized by the surface exposed peptide beta-hairpin loop on ERGIC-53 allowing for their removal from the ER.

The interaction data led me to believe that ERGIC-53 may be playing a role in “p97-UBXD1 complex dependent activities”. While the function of UBXD1 has remained largely unknown, p97 is known to play various roles within the cell that are regulated by adaptor binding. Given my previous data showing the p97^{UBXD1} interaction, I hypothesized that an UBXD1/ERGIC-53 interaction could play a role in further sorting and/or trafficking of ERGIC-53 complexes via a p97-dependent mechanism.

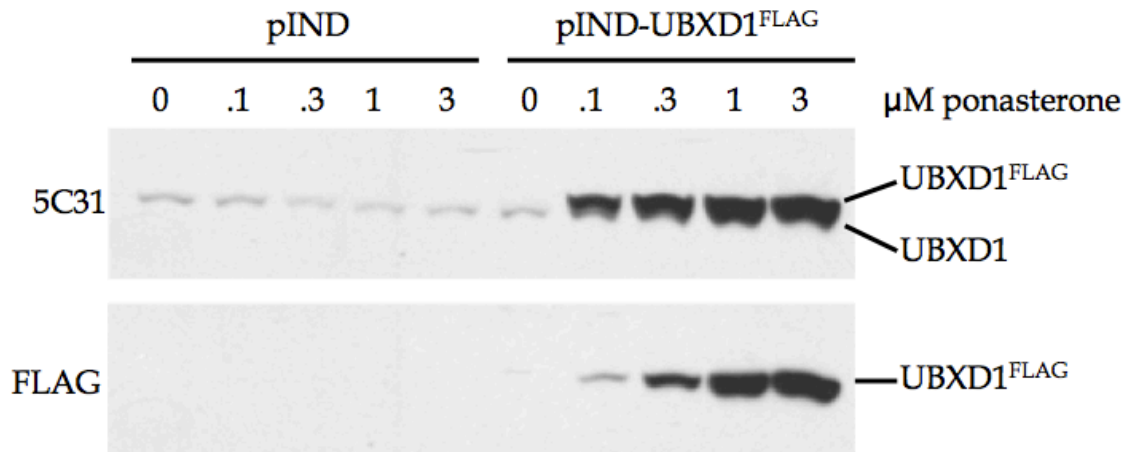


Figure 5. Ponasterone Inducible UBXD1^{FLAG} System. A cell line was generated to induce production of UBXD1^{FLAG} upon treatment with ponasterone. Cells were treated with .1, .3, 1 or 3μM ponasterone-containing media. After 24 hours of incubation, media was removed and replaced with fresh ponasterone-containing media for an additional 24 hours using the same concentrations as were previously used. After a total of 48 hours of induction, cells were harvested and lysed. Immunoprecipitations were carried out using anti-FLAG conjugated antibody and proteins were resolved by SDS-PAGE followed by transfer onto nitrocellulose membrane. Membranes were probed using anti-UBXD1 and anti-FLAG antibodies.

3.5 Verification of Proteomics Data by Western Blot Analysis

As a proof of principle, Figure 5 demonstrates induction of UBXD1^{FLAG} expression in a dose-dependent manner upon treatment of ponasterone in cells of the inducible cell line.

In order to verify the interaction data acquired by solution-based proteomics back at Temple, I used two different concentrations of ponasterone to induce UBXD1^{FLAG} expression in the inducible cell line. A concentration of .1 μ M was used to mimic production of UBXD1^{FLAG} at physiologically relevant levels and 3 μ M that resulted in an approximate 30-fold overexpression of UBXD1^{FLAG}. After induction, cells were harvested, extracts prepared, and immunoprecipitations carried out with anti-FLAG antibody conjugated beads. Immunoprecipitated proteins were resolved by SDS-PAGE then transferred to nitrocellulose membranes, which were probed with anti-FLAG and anti-ERGIC-53 antibodies. Endogenous ERGIC-53 was present in the anti-FLAG immunoprecipitates, including those derived from cells expressing UBXD1^{FLAG} at near physiologic levels(Figure 6).

As a point of interest, while in California, Dr. Haines wanted to determine the specificity of ERGIC-53 binding among other UBX-domain containing adaptors. Expression constructs encoding various FLAG-tagged p97 adaptor proteins were transiently transfected into H1299 cells. Immunoprecipitations using anti-FLAG antibody coupled beads and subsequent FLAG, ERGIC-53 and p97 western blots were performed as described above. Of the UBX-domain containing p97 adaptors tested, the results showed UBXD1 to be the only adaptor that interacted with ERGIC-53 (Figure 7).

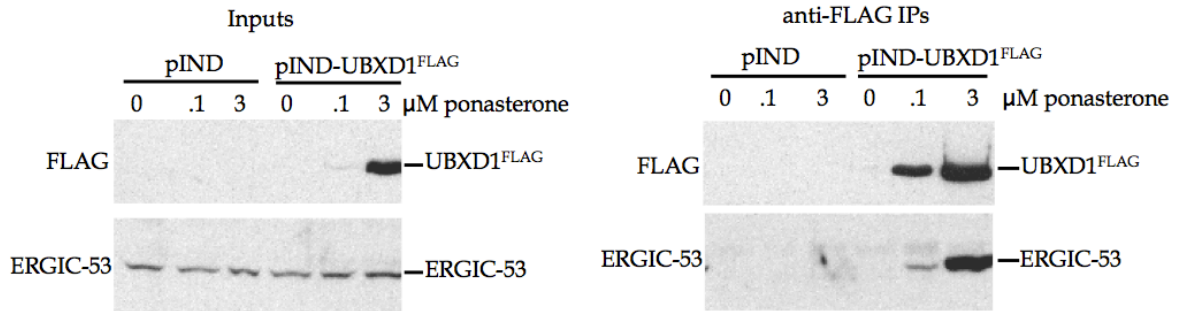


Figure 6. Inducible Expression of UBXD1^{FLAG} followed by anti-FLAG

Immunoprecipitation shows interaction with endogenous ERGIC-53. Two

different concentrations of ponasterone were used to induce UBXD1^{FLAG} expression in the inducible cell line. A concentration of .1μM was used to mimic production of UBXD1^{FLAG} at physiologically relevant levels and 3μM that resulted in an approximate 30-fold overexpression of UBXD1^{FLAG}. After 48 hours of induction in the presence of ponasterone, cells were harvested and lysed.

Immunoprecipitations were then carried out using anti-FLAG antibody conjugated beads. Immunoprecipitated proteins were resolved by SDS-PAGE then transferred to nitrocellulose membranes and probed with anti-FLAG and anti-ERGIC-53 antibodies.

Interestingly, it was observed that while the C-terminal FLAG-tagged UBXD1 expression construct was able to bind ERGIC-53, the N-terminal FLAG-tagged UBXD1 did not show any evidence of interaction with endogenous ERGIC-53.

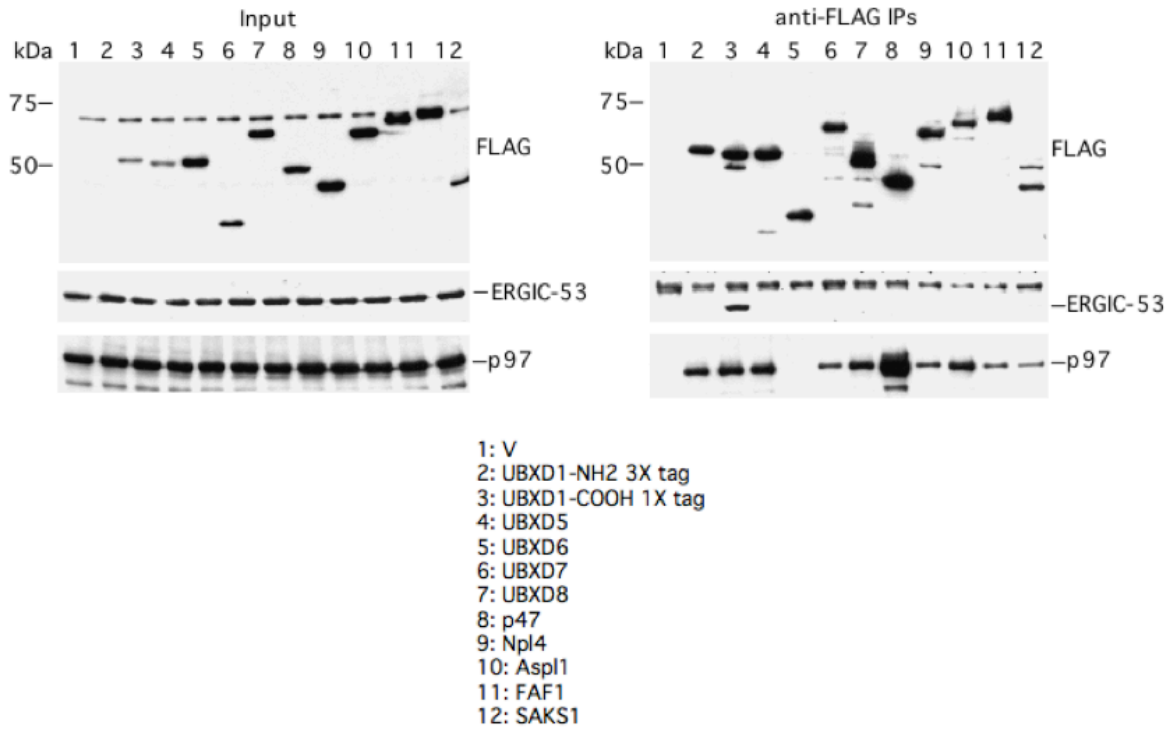


Figure 7. Specificity of ERGIC-53 binding among p97 adaptor proteins. H1299 cells were transiently transfected with expression constructs encoding the above FLAG-tagged p97 adaptor proteins. Immunoprecipitations were carried out using anti-FLAG antibody coupled beads. Proteins were resolved by SDS-PAGE and transferred to nitrocellulose membranes. Subsequent anti-FLAG, anti-ERGIC-53 and anti-p97 western blots were performed.

3.6 ERGIC-53 Interacts with the UBXD1 N-terminus

Since the C-terminal flag-tagged UBXD1 construct maintained the ability to interact with ERGIC-53, it was hypothesized that the UBXD1 N-terminus is required for ERGIC-53 binding. To address this, I performed interaction assays with a full-length UBXD1^{FLAG} expression construct and a UBXD1^{FLAG} expression construct lacking the first 50 amino acids of the N-terminus. H1299 cells were transiently transfected with these constructs followed by immunoprecipitations using anti-FLAG antibody conjugated beads. Immunoprecipitated proteins were resolved by SDS-PAGE then transferred to nitrocellulose membranes, which were probed with anti-FLAG and anti-ERGIC-53 antibodies. Deletion of the first 50 amino acids of the UBXD1 amino-terminus resulted in loss of ERGIC-53 binding. This result led me to believe that this region is critical for interaction between these two proteins(Figure 8).

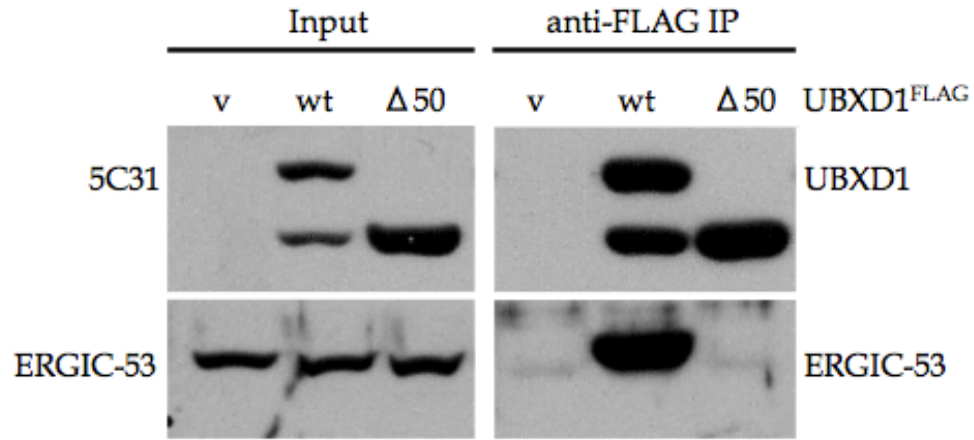


Figure 8. UBXD1 N-terminus is Required for ERGIC-53 Binding. H1299 cells were transiently transfected with these constructs followed by immunoprecipitations using anti-FLAG antibody conjugated beads. Immunoprecipitated proteins were resolved by SDS-PAGE then transferred to nitrocellulose membranes, which were probed with anti-FLAG and anti-ERGIC-53 antibodies.

3.7 The Cytoplasmic Tail of ERGIC-53 is Required for Binding to UBXD1

After identifying the novel UBXD1/ERGIC-53 interaction and determining the N-terminal region of UBXD1 as being required for binding, the ERGIC-53 domain necessary for interaction with UBXD1 remained unknown. Previous studies aimed at characterizing UBXD1 suggested approximately half of endogenous UBXD1 to exist in the peripheral membrane-associated state (Madsen et al., 2008). As highlighted previously, ERGIC-53 is present as an integral membrane protein within the lumen of the ER and contains a twelve amino acid cytosolic C-terminal tail. As this region of the protein is the only domain available to interact with other cytosolic proteins, I focused on the cytoplasmic tail of ERGIC-53 to determine if it was required for UBXD1 binding.

To test the requirement of this domain in binding to the UBXD1 N-terminus, I generated an amino-terminal FLAG-tagged ERGIC-53 mutant lacking the twelve amino acids that make up the cytoplasmic tail. HEK293T cells were transiently transfected followed by immunoprecipitation using anti-HA antibody conjugated beads. Immunoprecipitated proteins were resolved by SDS-PAGE then transferred to nitrocellulose membranes, which were probed with anti-FLAG, anti-ERGIC-53 and anti-UBXD1 antibodies. Results showed loss in the ability of UBXD1^{HA} to interact with ^{FLAG}ERGIC-53 in the absence of the C-terminal tail (Figure 9).

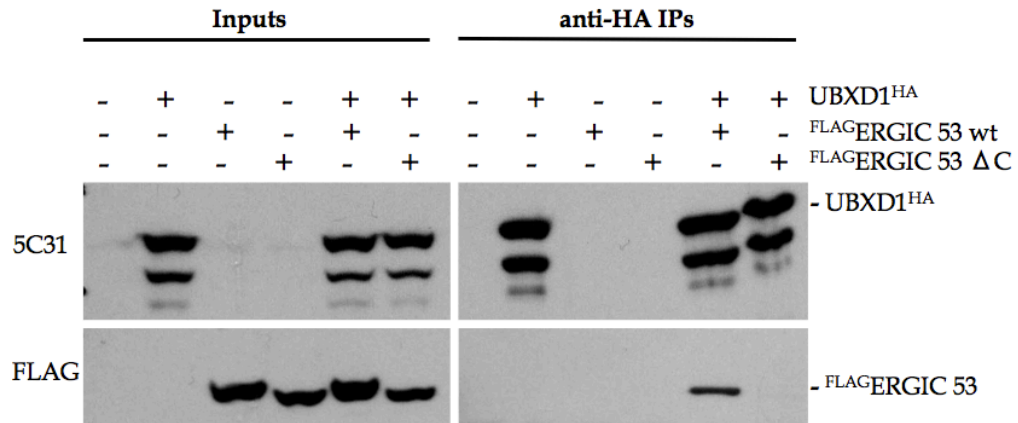


Figure 9. Requirement of the ERGIC-53 cytosolic tail for interaction with UBXD1. HEK293T cells were transiently transfected as noted above, followed by immunoprecipitation using anti-HA antibody conjugated beads. Immunoprecipitated proteins were resolved by SDS-PAGE and transferred to nitrocellulose membranes, which were probed with anti-FLAG and anti-UBXD1 antibodies.

Following the discovery of a novel interaction between UBXD1 and ERGIC-53 by Dr. Dale Haines, I was able to verify the proteomics data and demonstrate that presence of a N-terminal FLAG tag on UBXD1 abrogated the interaction between these proteins, leading to the discovery that the first ten amino-acids of the UBXD1 N-terminus are required for ERGIC-53 binding. Further investigation of this interaction allowed me to establish the requirement of the ERGIC-53 cytoplasmic tail for UBXD1 binding.

3.8 UBXD1 Interacts with the COPI β Subunit

The carboxy-terminal tail of ERGIC-53 interacts with proteins that control its intracellular trafficking. In particular, ERGIC-53 contains a C-terminal KKFF motif in which the di-phenylalanine residues have been shown to bind the coat protein complex II (COPII) to promote budding from the ER. Furthermore, the di-lysine residues are responsible for anterograde transport to the ER from the ERGIC and potentially other vesicles. When bound to adaptor proteins, p97 complexes are known to modulate protein interactions. Since UBXD1 was found to bind ERGIC-53, I wanted to determine if UBXD1 preferentially associated with proteins present in COPII or COPI complexes. Interestingly, I found that UBXD1 binds robustly to the COPI β subunit, but not the COPI γ subunit or the COPII member Sec22 (Figure 10). These results raise the possibility that the p97^{UBXD1} complex may modulate ERGIC-53 and/or COPI subunit interactions.

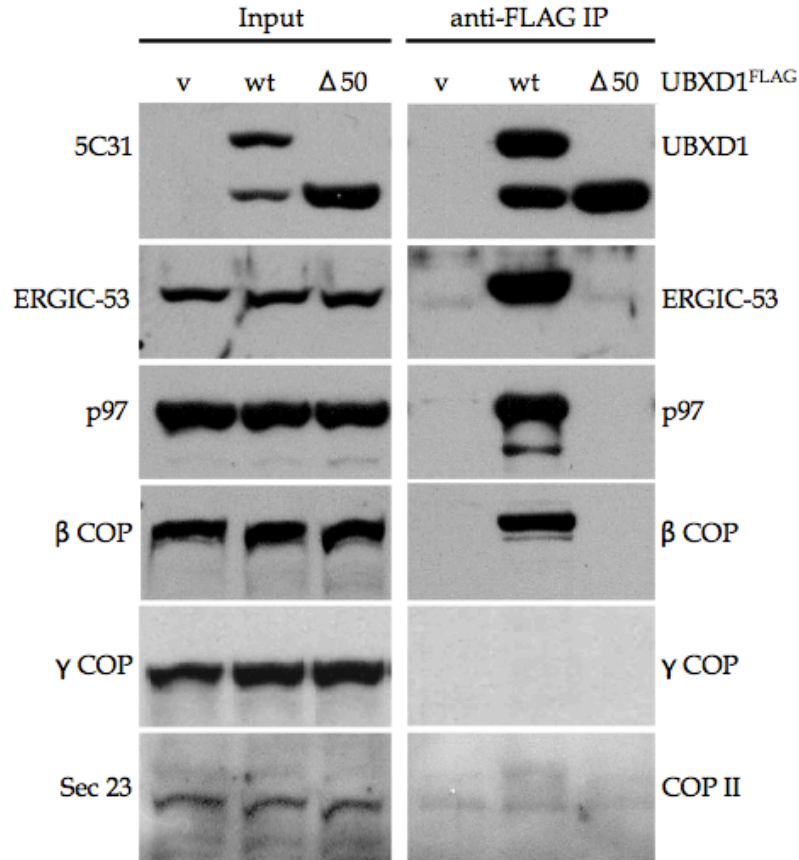


Figure 10. Ability of UBXD1^{FLAG} to co-immunoprecipitate COPI β subunit in addition to ERGIC-53 and p97. Cells were transiently transfected with UBXD1^{FLAG}, harvested 48 hours later and lysed. Immunoprecipitations were carried out using anti-FLAG antibody conjugated beads. Proteins were resolved using SDS-PAGE and transferred to nitrocellulose membrane, then probed using anti-UBXD1, anti-ERGIC-53, anti-p97, anti-βCOP, anti-γCOP and anti-Sec23 antibodies. Results show the ability of UBXD1^{FLAG} to bind βCOP robustly, but not the COPI γ subunit or the COPII member Sec22.

Given the exclusivity of ERGIC-53 binding to UBXD1 and not other UBX-domain containing p97 adaptors, I wanted to test if the same was true for β COP. Expression constructs encoding various FLAG-tagged p97 adaptor proteins were transiently transfected into H1299 cells. Immunoprecipitations using anti-FLAG antibody coupled beads and subsequent anti-FLAG, anti-p97 and anti- β COP western blots were performed as described above. Results showed that all UBX-domain containing p97 adaptors tested were capable of interacting with β COP (Figure 11), illustrating that the interaction is not exclusive to UBXD1.

Intriguingly, however, I observed a correlation between the amount of β COP and p97 being co-immunoprecipitated by the various adaptors. The results indicated that the amount of p97 interacting with FLAG-tagged adaptors was relative to the amount of β COP being co-immunoprecipitated. Based on this “mirrored pull-down” effect, I hypothesized that UBXD1 was indirectly interacting with the COPI β subunit via p97.

In order to confirm the hypothesis, I tested the ability of p97 to interact with COPI beta-subunit both in the presence and absence of UBXD1 using a miRNA based system created in H1299 cells to knockdown UBXD1 upon treatment with doxycycline. After 96 hours of culturing in the presence of doxycycline, cells were transiently transfected with ^{FLAG}p97 followed by immunoprecipitation using anti-FLAG antibody conjugated beads. Proteins were then resolved by SDS-PAGE, transferred to a nitrocellulose membrane and probed with anti-p97, anti-beta COP and anti-UBXD1 antibodies. Results of the experiment showed the ability of p97 to interact with the COPI β subunit upon knockdown of UBXD1 (Figure 12).

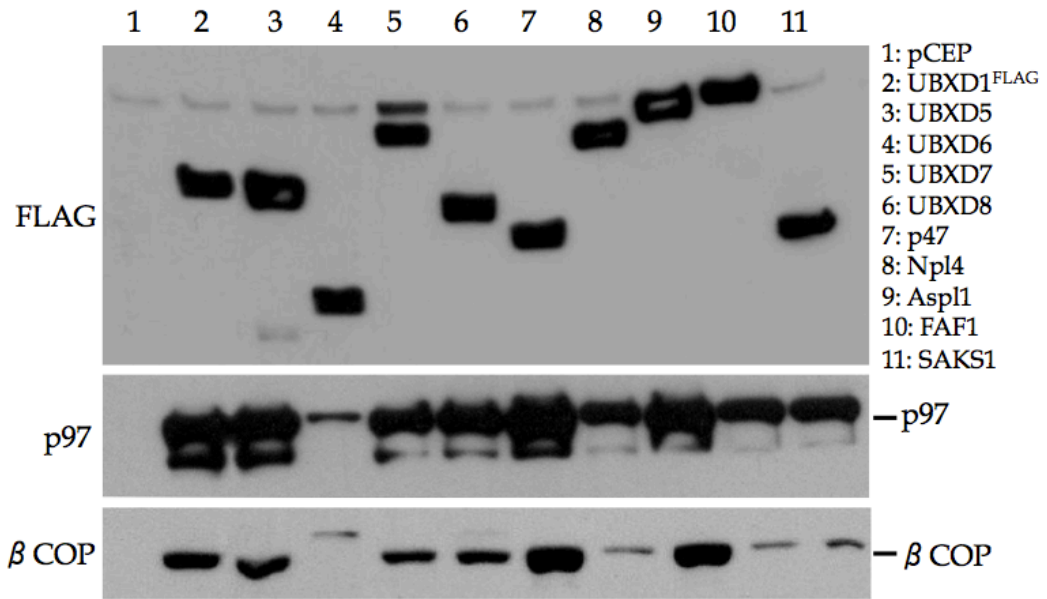


Figure 11. Mirrored Pulldown of p97 and βCOP using FLAG-tagged p97 adaptors. Expression constructs encoding various FLAG-tagged p97 adaptor proteins were transiently transfected into H1299 cells. Immunoprecipitations using anti-FLAG antibody coupled beads. Proteins were resolved by SDS-PAGE, transferred to nitrocellulose membrane, which were probed with anti-FLAG, anti-p97 and anti-βCOP antibodies.

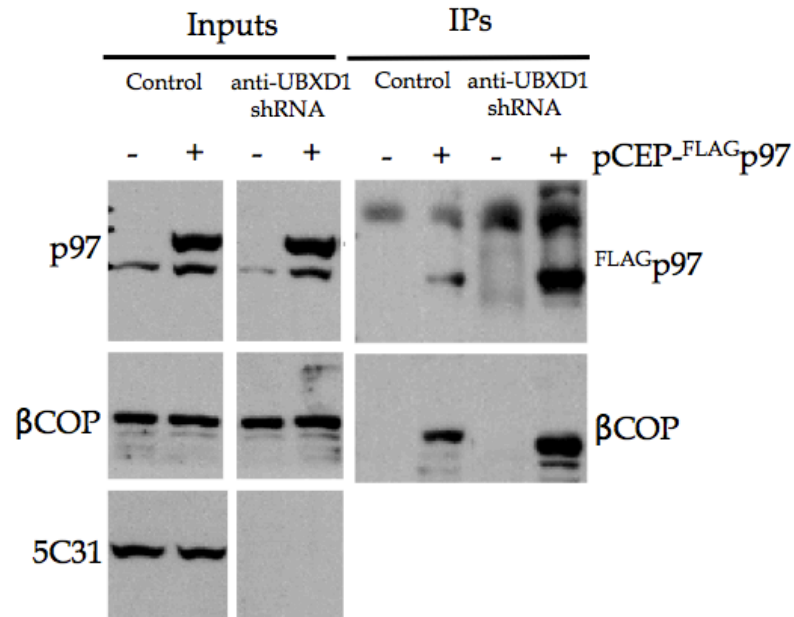


Figure 12. p97/ β COP Interaction in the Presence and Absence of UBXD1.

After 96 hours of culturing in the presence of doxycycline, cells were transiently transfected with ^{FLAG}p97 followed by immunoprecipitation using anti-FLAG antibody conjugated beads. Proteins were then resolved by SDS-PAGE, transferred to a nitrocellulose membrane and probed with anti-p97, anti-beta COP and anti-UBXD1 antibodies.

Although the significance of this interaction is not yet known, these two proteins have been shown to work closely in mediating vesicular budding and membrane fusion events(Tang et al., 2008). In the discussion, I will speculate on possible models that support this interaction including the involvement of ERGIC-53 and UBXD1.

CHAPTER 4

DISCUSSION

Single nucleotide polymorphisms (SNPs) are characterized as a variation in the DNA sequence between biological species where a single nucleotide is exchanged for another. It is estimated that the human genome contains at least 11 million SNPs, with approximately 7 million of these occurring with a minor allele frequency greater than 5% and the rest between 1-5%. To be considered valid, a SNP must be present within at least 1% of the population ($MAF \geq 1\%$). The region of the genome in which this polymorphism occurs determines the severity of this sequence alteration. Approximately 3% of the human genome encodes protein. If an SNP occurs outside of a protein-coding region, it is far less likely to result in an alteration of normal biological function. However, a SNP occurring within exons, promoters or other important regions of the genome can have mild to severe consequences including protein misfolding, loss of function, introduction of premature stop codons and alternative splice sites. As the idea of personalized medicine becomes increasingly more popular, SNPs are being studied closely to assess their contribution to disease progression and how different individuals respond to certain treatments. The availability of the human genome reference sequence has made it possible to begin the search for patterns and frequencies of SNPs between individuals. Genome-wide association studies (GWAS) have contributed greatly to identifying the statistical association between hundreds of loci across the genome and common complex traits. Unfortunately, this approach

limits the ability to associate SNPs between populations and is not sophisticated enough to provide information about rare variants. Current and future research is dedicated to improving these analytical methods to further understand and characterize rare SNPs.

Presence of the UBXD1 N184S SNP within the Japanese SNP database in combination with my observation that this polymorphic variant showed a severe reduction in p97 binding prompted me to validate the SNP by determining its prevalence using placental DNA for various ethnic backgrounds as my sample population. The UBXD1 N184S SNP was originally identified using genomic DNA from twenty-four unrelated Japanese female volunteers. My inability to confirm this SNP within the sample population could be the result of two different scenarios. First, although present within the database, the N/S polymorphism could be rare, making the sample size of fifty-three people too small to properly analyze its frequency with proper accuracy. Ideally a larger, more ethnically focused sample population should be considered in order for the findings to be significant. Unfortunately, I was limited by the lack of ethnic diversity and number of samples that could be obtained in addition to a lack of resources to make such a feat practical.

Another possibility is that the SNP could have been erroneously introduced as a result of infidelity by the polymerase or suboptimal buffer condition used in the PCR reaction. On average, the error-rate frequency of PCR polymerases ranges from 1.3×10^{-6} to 5×10^{-5} . Use of a low fidelity polymerase increases the error rate approximately 5-30 fold over that of high fidelity polymerase (Cline et al., 1996).

While the group that originally characterized the UBXD1 N184S SNP reported using a high fidelity *Pfu* polymerase, the possibility of PCR-introduced error still exists although it is much less likely.

While I was unable to verify the UBXD1 N184S SNP, the interaction data showing a severe loss in p97 binding remained convincing. As noted, the function of p97 is dictated by the binding of adaptor proteins, which are known to modulate the function of p97 in a variety of cellular processes. The importance of these adaptor proteins in proper p97 function can be observed upon mutation of key residues responsible for interaction with p97. While *in vivo* mutation of p97 adaptor proteins has not yet been linked to improper p97 function, previous reports have indicated the presence of mutations within the N-terminal domain of p97 can drastically affect adaptor binding, leading to pathologies associated with the inability to degrade aggregate-prone proteins. Such 'proteinopathies' include inclusion body myopathy with Paget disease of bone and frontotemporal dementia (IBMPFD), Parkinson's Disease, Alzheimer's Disease and polyglutamate diseases. In a 2010 report, Buchberger and Fernandez-Saiz proposed that mutations harbored within the N-terminal domain of p97 induce conformational alterations that interfere with communication between the N and D1 domains, thus disturbing co-factor binding. As a result, it was suggested that impairment in degradation of p97 target proteins could lead to a build-up of ubiquitinated protein aggregates. The Haines laboratory has unpublished data indicating that UBXD1 is defective at binding p97 mutants found in IBMPFD as well as ALS in addition to data that supports a positive role for UBXD1 in autophagy. If this turns out to be the case, it

will be worthwhile to sequence more individuals to determine if the UBXD1 N184S SNP is indeed a valid polymorphism. If proven valid, it will be interesting to investigate whether individuals harboring this SNP are more prone to develop neurological diseases that show defects in clearance of misfolded proteins by autophagy.

At least for now, the role UBXD1 plays in autophagy and perhaps other cellular pathways remains unclear. Using mass spectroscopy-based proteomics, I hoped to gain insight into the biological function of UBXD1 by analyzing protein interaction profiles. However, this method requires samples to be electrophoresed through a gel matrix and excised in order to be analyzed and has proven to be very difficult as trace contaminations from other fractions are often present.

Additionally, sub-optimal lysis conditions leading to loss of interactions can be misleading when interpreting results. In the end, band excision followed by mass spectroscopy-based proteomics did not yield any convincing data to help identify UBXD1 interacting proteins.

In contrast to these results, the more elegant and sophisticated solution-based proteomics approach yielded useful information as it identified ERGIC-53 to be a novel UBXD1 interacting partner.

ERGIC-53 is a non-glycosylated type-I single spanning trans-membrane protein that is localized to the ER-Golgi intermediate compartment (ERGIC) where it serves as a transporter of glycoprotein clients between the ER, ERGIC and cis-Golgi in the early secretory pathway. Present as a hexamer, ERGIC-53 contains a short cytoplasmic tail domain containing a C-terminal KKFF motif required for proper

targeting of the protein within the ER-ERGIC-Golgi pathway, a trans-membrane domain, a stalk region containing two cysteines required for oligomerization, a carbohydrate recognition domain required for interaction with its client proteins and an amino terminal region. The process of client transport and ERGIC-53 recycling occurs through the following general steps. Newly synthesized ERGIC-53 monomers translocate to the lumen of the rough ER and oligomerize to form homohexameric ERGIC-53 capable of binding clients. Client-bound ERGIC-53 containing vesicles bud from the ER membrane in a COPII dependent manner upon activation of the guanine nucleotide binding protein, Arf1. COPII vesicles bind to the ERGIC-53 C-terminal di-phenylalanine motif, which is required for proper transport of client-bound ERGIC-53 to the ERGIC. After release of clients, ERGIC-53 recycles back to the ER via COPI coated vesicles that bind a C-terminal di-lysine motif upon Arf1 activation. ERGIC-53 is also thought to recycle back from the early endosome in the same manner.

Elucidation of the domains responsible for the UBXD1/ERGIC-53 interaction was crucial so that future functional studies could be performed to further characterize this novel interaction. Through generation of a UBXD1 N-terminal deletion mutant, I was able to discern the general domain required for the interaction between UBXD1 and ERGIC-53. Inversely, deletion of the ERGIC-53 C-terminal tail showed loss of UBXD1 binding. Together, these results confirm my previous hypothesis that the N-terminal domain of UBXD1 interacts with ERGIC-53 and the cytoplasmic tail of ERGIC-53 is required for interaction with UBXD1. To expand on these results, recent unpublished data generated within the Haines Lab

has shown loss of ERGIC-53 binding upon deletion of the first ten amino acids of the UBXD1 N-terminus. Furthermore, UBXD1 N-terminal point mutants have helped determine the specific amino acids required for this interaction. Future analysis using ERGIC-53 C-terminal point mutants will have to be performed to determine what specific residues within the ERGIC-53 cytoplasmic tail required for binding UBXD1.

Previous studies in the laboratory have shown a robust p97^{UBXD1} interaction, allowing me to speculate that UBXD1 binding to ERGIC-53 could play a role in further sorting and/or trafficking of ERGIC-53 complexes via a p97-dependent mechanism. Considering that p97 has been shown to regulate protein-protein interactions when bound to adaptor proteins, I wanted to test if the p97^{UBXD1} was able to interact members of ERGIC-53 containing complexes. Through UBXD1^{FLAG} immunoprecipitation, I was able to co-immunoprecipitate the COPI beta subunit in addition to ERGIC-53 and p97. Interestingly, however, I was able to demonstrate a robust interaction between ^{FLAG}p97 and endogenous β COP in the absence of UBXD1. This leads me to speculate that UBXD1 interacts with β COP in a p97 dependent manner. A hypothetical model illustrating these interactions is shown in Figure 13.

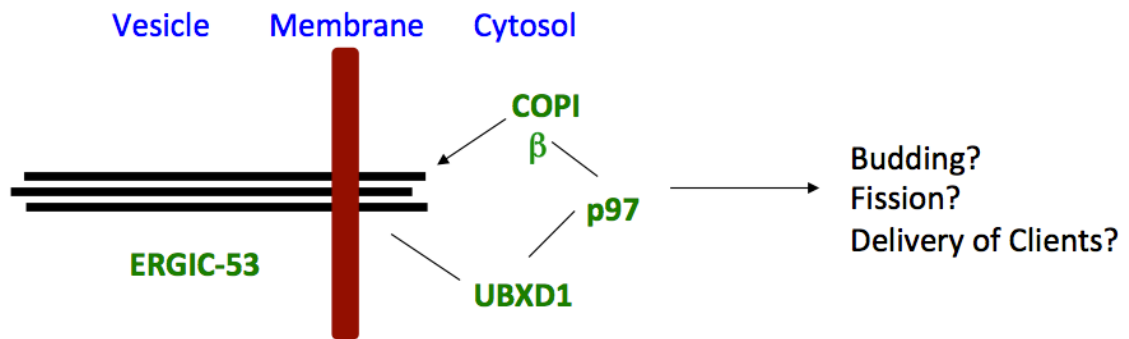


Figure 13. Model for UBXD1 interaction with β COP in a p97 dependent manner. Hypothetical model based on interaction data and possible functional outcomes of these interactions.

Why the $p97^{UBXD1}$ complex preferentially interacts with the COPI beta subunit but not other COPI subunits remains unclear. It is possible that this complex plays a role in the remodeling of COPI complexes based on the contents of COPI coated vesicles. Or, remodeling of the coatomeer coat composition by the $p97^{UBXD1}$ complex could be a way of determining vesicles to specific pathways.

COPI complexes have also been implicated as being required for proper maturation of early endosomes. Moreover, morphological evidence supports the fusion of early endosomes with autophagic vacuoles for proper functioning of autophagy. Curiously, similar to the expression of p97 mutants found in IBMPFD and ALS, siRNA mediated knockdown of β COP, β' COP or α COP shows accumulation of GFP-LC3+ autophagic vacuoles that are not degradative. Also, knockdown of these COPI subunits results in accumulation of p62/SQSTM1 structures as well as ubiquitin and ubiquitin labeled vesicular structures (Razi et al., 2009). It is thought that fusion of autophagic vacuoles with early endosomes could provide the targeting machinery necessary for vacuole fusion with the later compartments. However,

how the autophagic vacuoles are initially targeted to fuse with early endosomes remains to be determined. Based on the available data, current speculation within the lab is that p97, in collaboration with UBXD1, modulates ERGIC-53 and COPI complex interactions at the ERGIC or early endosome and this activity is required for the movement of proteins involved in autophagosome-lysosome fusion.

REFERENCES CITED

- Acharya U, Jacobs R, Peters JM, Watson N, Farquhar MG, Malhotra V. (1995). The formation of Golgi stacks from vesiculated Golgi membranes requires two distinct fusion events. *Cell* **82**, 895-904.
- Allen MD, Buchberger A, Bycroft M. (2006). The PUB domain functions as a p97 binding module in human peptide N-glycanase. *J. Biol. Chem.* **281**, 25502-8.
- Beuron, F., Flynn, T.C., Ma, J., Kondo, H., Zhang, X., Freemont, P.S. (2003). Motions and negative cooperativity between p97 domains revealed by cryo-electron microscopy and quantised elastic deformational model. *J. Mol. Biol.* **327**, 619–629.
- Cline J, Braman JC, Hogrefe HH. (1996). PCR fidelity of pfu DNA polymerase and other thermostable DNA polymerases. *Nucleic Acids Res.* **15**, 3546-51.
- Dai, R.M., Li, C.C. (2001). Valosin-containing protein is a multi-ubiquitin chain-targeting factor required in ubiquitin–proteasome degradation. *Nat. Cell Biol.* **3**, 740–744.
- DeLaBarre B, Christianson JC, Kopito RR, Brunger AT. (2006). Central pore residues mediate the p97/VCP activity required for ERAD. *Mol. Cell* **22**, 451-62.

Dreveny, I., Kondo, H., Uchiyama, K., Shaw, A., Zhang, X., Freemont, P. S. (2004). Structural basis of the interaction between the AAA ATPase p97/VCP and its adaptor protein p47. *Embo J.* **23**, 1030–1039.

Egerton, M., Ashe, O.R., Chen, D., Druker, B.J., Burgess, W.H., Samelson, L.E. (1992). VCP, the mammalian homolog of cdc48, is tyrosine phosphorylated in response to T cell antigen receptor activation. *EMBO J.* **11**, 3533–3540.

Egerton, M., Samelson, L.E. (1994). Biochemical characterization of valosin-containing protein, a protein tyrosine kinase substrate in hematopoietic cells. *J. Biol. Chem.* **269**, 11435–11441.

Ficarro, S., Chertihin, O., Westbrook, V.A., White, F., Jayes, F., Kalab, P., Marto, J.A., Shabanowitz, J., Herr, J.C., Hunt, D.F., Visconti, P.E. (2003). Phosphoproteome analysis of capacitated human sperm. Evidence of tyrosine phosphorylation of a kinase-anchoring protein 3 and valosin-containing protein/p97 during capacitation. *J. Biol. Chem.* **278**, 11579–11589.

Haga H, Yamada R, Ohnishi Y, Nakamura Y, Tanaka T. (2002). Gene-based SNP discovery as part of the Japanese Millennium Genome Project: identification of 190,562 genetic variations in the human genome. Single-nucleotide polymorphism. *J. Hum. Genet.* **47**, 605-10.

Kappeler F, Klopfenstein DR, Foguet M, Paccaud JP, Hauri HP. (1997). The recycling of ERGIC-53 in the early secretory pathway. ERGIC-53 carries a cytosolic endoplasmic reticulum-exit determinant interacting with COPII. *J. Biol. Chem.* **272**, 31801-8.

Kern M, Fernandez-Sáiz V, Schäfer Z, Buchberger A. (2009). UBXD1 binds p97 through two independent binding sites. *Biochem Biophys Res Commun.* **380**, 303-7.

Latterich M, Fröhlich KU, Schekman R. (1995). Membrane fusion and the cell cycle: Cdc48p participates in the fusion of ER membranes. *Cell* **82**, 885-93.

Madsen L, Andersen K.M., Prag S., Moos T., Semple C.A., Seeger M., Hartmann-Petersen R. (2008). Ubx1 is a novel co-factor of the human p97 ATPase. *Int J Biochem Cell Biol.* **40**, 2927-42.

Nichols WC, Terry VH, Wheatley MA, Yang A, Zivelin A, Ciavarella N, Stefanile C, Matsushita T, Saito H, de Bosch NB, Ruiz-Saez A, Torres A, Thompson AR, Feinstein DI, White GC, Negrier C, Vinciguerra C, Aktan M, Kaufman RJ, Ginsburg D, Seligsohn U. (1999). ERGIC-53 gene structure and mutation analysis in 19 combined factors V and VIII deficiency families. *Blood.* **93**, 2261-6.

Rabouille C, Levine TP, Peters JM, Warren G. (1995). An NSF-like ATPase, p97, and NSF mediate cisternal regrowth from mitotic Golgi fragments. *Cell* **82**, 905-14.

Rouiller, I., DeLaBarre, B., May, A.P., Weis, W.I., Brunger, A.T., Milligan, R.A., Wilson-Kubalek, E.M. (2002). Conformational changes of the multifunction p97 AAA ATPase during its ATPase cycle. *Nat. Struct. Biol.* **9**, 950–957.

Schuberth C, Buchberger A. (2008). UBX domain proteins: major regulators of the AAA ATPase Cdc48/p97. *Cell Mol. Life Sci.* **65**, 2360-71.

Suzuki T, Kitajima K, Emori Y, Inoue Y, Inoue S. (1997). Site-specific de-N-glycosylation of diglycosylated ovalbumin in hen oviduct by endogenous peptide: N-glycanase as a quality control system for newly synthesized proteins. *Proc. Natl. Acad. Sci.* **94**, 6244-9.

Suzuki T, Park H, Till E.A., Lennarz W.J. (2001). The PUB domain: a putative protein-protein interaction domain implicated in the ubiquitin-proteasome pathway. *Biochem. Biophys. Res. Commun.* **12**, 1083-7.

Tang D, Mar K, Warren G, Wang Y. (2008). Molecular mechanism of mitotic Golgi disassembly and reassembly revealed by a defined reconstitution assay. *J. Biol. Chem.* **283**, 6085-94.

Tresse E, Salomons FA, Vesa J, Bott LC, Kimonis V, Yao TP, Dantuma NP, Taylor JP. (2010). VCP/p97 is essential for maturation of ubiquitin-containing

autophagosomes and this function is impaired by mutations that cause IBMPFD. *Autophagy*. **6**, 217-27.

Wang, Q., Song, C., Li, C.C. (2003). Hexamerization of p97-VCP is promoted by ATP binding to the D1 domain and required for ATPase and biological activities. *Biochem. Biophys. Res. Commun.* **300**, 253–260.

Wang, Q., Song, C., Yang, X., Li, C.C. (2003). D1 ring is stable and nucleotide-independent, whereas D2 ring undergoes major conformational changes during the ATPase cycle of p97-VCP. *J. Biol. Chem.* **278**, 32784–32793.

Wang Q, Song C, Li CC. (2004). Molecular perspectives on p97-VCP: progress in understanding its structure and diverse biological functions. *J. Struct. Biol.* **146**, 44-57.

Wójcik C, Yano M, DeMartino GN. (2004). RNA interference of valosin-containing protein (VCP/p97) reveals multiple cellular roles linked to ubiquitin/proteasome-dependent proteolysis. *J. Cell Sci.* **117**, 281-92.

Zhang,X., Shaw,A., Bates,P.A., Newman,R.H., Gowen,B., Orlova, E., Gorman, M.A., Kondo, H., Dokurno, P., Lally, J., Leonard, G., Meyer, H., van Heel, M., Freemont, P.S. (2000). Structure of the AAA ATPase p97. *Mol. Cell* **6**, 1473–1484.

Zhao G., Zhou X., Wang L., Li G., Schindelin H., Lennarz W.J. (2007). Studies on peptide:N-glycanase-p97 interaction suggest that p97 phosphorylation modulates endoplasmic reticulum-associated degradation. *Proc Natl Acad Sci.* **104**, 8785-90.